Effect of Natural L- to D-Amino Acid Conversion on the Organization, Membrane Binding, and Biological Function of the Antimicrobial Peptides Bombinins H[†]

Maria Luisa Mangoni,*,[‡] Niv Papo,[§] José M. Saugar,[‖] Donatella Barra,[‡,⊥] Yechiel Shai,[§] Maurizio Simmaco,[‡] and Luis Rivas*,[‖]

Istituto Pasteur-Fondazione Cenci Bolognetti, Dipartimento di Scienze Biochimiche 'A. Rossi Fanelli', Azienda Ospedaliera S. Andrea, and CNR Istituto di Biologia e Patologia Molecolari, Università 'La Sapienza', Piazzale Aldo Moro 5, 00185 Rome, Italy, Department of Biological Chemistry, The Weizmann Institute of Science, Rehovot 76100, Israel, and Centro de Investigaciones Biologicas, Ramiro de Maeztu 9, E-28040 Madrid, Spain

ABSTRACT: Antimicrobial peptides (AMPs) are evolutionarily old components of innate immunity found in all living pluricellular organisms. Interestingly, some organisms express families of AMPs with only a slight variation among their members, possibly to increase their spectrum of activity. Despite the growing body of knowledge about their biological activity and mode of action on bacteria, only a few of them have been tested on *Leishmania*, a worldwide spread protozoan pathogen, and the parameters contributing to this activity are yet to be determined. We report on the anti-*Leishmania* activity and mode of action of bombinins H2 and H4 isolated from the skin secretion of the frog *Bombina variegata*. H4, the most active, is the first natural AMP of animal origin with a single L- to D-amino acid isomerization. Membrane depolarization and membrane permeation assays, as well as electron microscopy, suggest that the lethal mechanism involves plasma membrane permeation and/or disruption. To better understand the enhanced activity of H4, we determined the peptide's structure in membranes mimicking those of mammals, bacteria, and *Leishmania* by using ATR-FTIR and CD spectroscopies and assessed their membrane binding by using surface plasmon resonance. The data reveal that (i) H2 but not H4 partially aggregates in membranes mimicking those of *Leishmania*, (ii) H2 is slightly more helical than H4 in all membranes, and (iii) H4 binds the *Leishmania* model membrane ∼5-fold better than H2. This study highlights the importance of a single α-amino acid epimerization as a tool used by nature to modulate the activity of AMPs. In addition, our findings suggest bombinins H as potential templates for the development of new drugs with a new mode of action against *Leishmania*.

Gene-encoded antimicrobial peptides (AMPs)[1] are a principal constituent of the innate immunity in pluricellular organisms, with a ubiquitous distribution throughout the different zoological phyla, where they act as an initial barrier against invading microorganisms (reviewed in refs *1−4*). AMPs are characterized by a wide variety of structural and conformational features, but most of them are cationic and have a tendency to adopt amphipathic structures upon interacting with the membrane of the pathogens. The lethal mechanism underlying many of them involves the disruption of the cytoplasmic membrane of the target cell, with a subsequent loss of intracellular homeostasis. Because of their cationic character, they bind better to acidic phospholipids located on the membrane of prokaryotes and lower eukaryotes but absent in cells of higher eukaryotes (reviewed in refs *3* and *5*; see also ref *6* for alternative intracellular targets). The presence of additional extracellular barriers, such as the outer membrane and the peptidoglycan layer in bacteria, or the anionic cell wall in lower eukaryotes, imposes on AMPs an additional barrier to traverse in attempting to reach the cytoplasmic membrane (*7−11*). At present, more than 800

* To whom correspondence should be addressed. L.R.: Centro de Investigaciones Biológicas (CSIC), Ramiro de Maeztu 9, E-28040 Madrid, Spain; phone, +34-918373112; fax, +34-915360432; e-mail, luis.rivas@cib.csic.es. M.L.M.: Dipartimento di Scienze Biochimiche, Università La Sapienza, Piazzale Aldo Moro, 5, 00185 Roma, Italy; phone, +39-06337 75457; fax, +39 0633775405; e-mail, marialuisa.mangoni@uniroma1.it.

[‡] Istituto Pasteur-Fondazione Cenci Bolognetti, Dipartimento di Scienze Biochimiche 'A. Rossi Fanelli', Azienda Ospedaliera S. Andrea, Università 'La Sapienza'.

[§] The Weizmann Institute of Science.

[‖] Centro de Investigaciones Biologicas.

[⊥] CNR Istituto di Biologia e Patologia Molecolari, Università 'La Sapienza'.

[1] Abbreviations: AMP, antimicrobial peptide; bisoxonol, bis(1,3-diethylthiobarbituric)trimethine oxonol; CA(1−8)M(1−18), cecropin A−melittin hybrid (KWKLFKKIGIGAVLKVLTTGLPALIS-NH₂); cho, cholesterol; erg, ergosterol; Hanks+Glc, Hanks balanced salt medium with 20 mM D-glucose; HIFCS, heat-inactivated fetal calf serum; LPG, lipophosphoglycan; MTT, 3-(4,5-dimethylthiazol-2-yl)-2,5-diphenyltetrazolium bromide; OG, octyl glucoside; PBS, phosphate-buffered saline; PC, phosphatidylcholine; PE, phosphatidylethanolamine; PG, phosphatidylglycerol; PI, phosphatidylinositol; PS, phosphatidylserine; SPR, surface plasmon resonance.

sequences of AMPs have been reported (see http://www.bbcm.univ.trieste.it/~tossi/pag1.htm for a compilation regularly updated). In particular, the amphibian skin secretions constitute one of the richest sources wherein the peptides are synthesized and stored within granules of holocrine-type serous glands and released upon stimulation (*12−15*).

The skin secretions of *Bombina* species contain two families of AMPs: bombinins and the relatively hydrophobic bombinins H (*16−18*). Interestingly, the second N-terminal position of two of them, bombinins H4 and H7, bears a D-alloisoleucine residue, and they coexist with their corresponding all-L counterparts, bombinins H2 and H6, respectively (*18*). H4 and H7 are the first natural AMPs of animal origin having a D-amino acid resulting from a post-translational modification (*19, 20*), and the enzyme responsible for this L−D isomerization was recently isolated and characterized (*21*). The sequence of H2 is IIGPVLGLVG-SALGGLLKKI-NH$_2$. Preliminary experiments revealed that the D-amino acid containing bombinins H had consistently higher bactericidal and fungicidal activity, the reason for which was not clear (*22*). The positioning of the D-amino acid close to the N-terminus seems to minimize the possible impact caused by this epimerization on the average helicity of the peptide, known to be an important parameter for the antimicrobial activity and selectivity of AMPs (*5*).

Despite their ability to kill a broad spectrum of microorganisms, only a few AMPs have been assayed against *Leishmania*, and those few act mainly on promastigotes (the insect stage of the parasite). Leishmaniasis is an infectious disease with a global incidence of 10−12 million people infected (*23*), but the efficacy of the first-line drugs is increasingly being challenged by the growing incidence of multiresistant isolates (*24, 25*). *Leishmania* represents an attractive species for AMPs, both for mode of action studies and as a potential target. *Leishmania* has two unique characteristics. First, its plasma membrane is extremely resistant to mechanical stress, due to a subpellicular layer of microtubules beneath the plasma membrane, common to other trypanosomatids (*26, 27*). Second, its survival in harsh environments (sandfly gut or parasitophorus vacuole in the macrophage) requires a very high resistance against chemical and biological agents, partially provided by a well-developed glycocalyx (*28*) and by other factors not yet completely unveiled. The composition of the plasma membrane is also strongly modified during the life cycle of the parasite (*28*). The dependence of the activity of the AMPs with respect to the stage of *Leishmania* has been previously reported for the cecropin A−melittin hybrids (*8, 29*).

Here we investigate the leishmanicidal activity and a plausible mode of action of bombinins H2 and H4 on both promastigotes and amastigotes (the mammalian intracellular stage of the parasite) and on model phospholipid membranes. The results reveal the higher activity of H4 compared with that of H2 and are discussed with regard to the peptides' structure, their membrane binding, and their organization within membranes with different phospholipid compositions. Besides highlighting the importance of a single α-amino acid epimerization as a tool used by nature to modulate the activity of AMPs, our findings suggest bombinins H as potential templates for the development of new anti-*Leishmania* drugs with a new mode of action.

MATERIALS AND METHODS

Reagents and Peptides. Bis(1,3-diethylthiobarbituric)-trimethine oxonol (bisoxonol) and SYTOX Green were obtained from Molecular Probes (Leiden, The Netherlands). Bombinins H2 and H4 were purchased from SYNT:EM (Nîmes, France). The purity of the peptides was assessed by HPLC analysis and Edman degradation, and their concentrations were determined by amino acid analysis, as previously described (*30*). Phosphatidylcholine (PC) from egg yolk, phosphatidylethanolamine (PE) from *Escherichia coli*, phosphatidylinositol (PI) from bovine liver, phosphatidylglycerol (PG), cholesterol (cho), and ergosterol (erg) were purchased from Sigma. Phosphatidylserine (PS) from bovine spinal cord (sodium salt grade I) was purchased from Lipid Products (South Nutfield, U.K.). Other reagents, of the highest quality available, were obtained from Sigma (St. Louis, MO) or Merck (Darmstadt, Germany).

Preparation of Small Unilamellar Vesicles (SUVs). SUVs were prepared by sonication of PC/cho (10:1, w/w) or PE/PG (7:3, w/w) dispersions as previously described (*31*). Vesicles were visualized using a JEOL JEM 100B electron microscope (Japan Electron Optics Laboratory Co., Tokyo, Japan) as follows. A drop of vesicles was deposited on a carbon-coated grid and negatively stained with uranyl acetate. Examination of the grids demonstrated that the vesicles were unilamellar with an average diameter of 20−50 nm.

Parasites. Promastigotes of *Leishmania donovani* (MHOM/SD/00/1S-2D) were grown in RPMI-1640 medium (Gibco, Paisley, U.K.) supplemented with 10% heat-inactivated fetal calf serum (HIFCS), gentamycin, penicillin, and 2 mM glutamine, placed in a Bellco roller device (Ace Glass, Vineland, NJ) at 26 °C. The mutant R2D2 strain, defective in the biosynthesis of the repetitive phosphorylated disaccharide unit of lipophosphoglycan (LPG), was kindly provided by S. J. Turco (School of Medicine, University of Kentucky, Lexington, KY). For this strain, 5 μg/mL lectin ricin agglutinin (*Ricinus communis*) was added to the growth medium (*32*). *Leishmania pifanoi* axenic amastigotes (MHOM/VE/60Ltrod) were grown at 32 °C in M199 medium (Gibco-BRL 31100) supplemented with 20% HIFCS, 5% trypticase, and 50 μg/mL hemin (pH 7.2) (*33*).

Activity of the Peptides on Leishmania Promastigotes and Amastigotes. Procyclic promastigotes and amastigotes were harvested at a late exponential phase of growth, washed twice with Hanks medium [136 mM NaCl, 4.2 mM Na$_2$HPO$_4$, 4.4 mM KH$_2$PO$_4$, 5.4 mM KCl, and 4.1 mM NaHCO$_3$ (pH 7.2)] (*34*), supplemented with 20 mM D-glucose (Hanks+Glc), and resuspended in the same buffer at a final concentration of 2 × 10^7 parasites/mL. Aliquots of this suspension (120 μL) were incubated with the peptides for 60 min, at either 26 or 32 °C for promastigotes or amastigotes, respectively, and subsequently split into two aliquots of 100 and 10 μL, used in the following two assays (*8*).

(i) The inhibition of 3-(4,5-dimethylthiazol-2-yl)-2,5-diphenyltetrazolium bromide (MTT) reduction to insoluble formazan by mitochondrial reductases was used as a short-term parameter of parasite viability and assayed immediately after peptide incubation (*29*). To the 100 μL aliquot of the parasite suspension incubated with the peptide was added 1 mL of Hanks+Glc to slow the peptide activity. The parasites were then collected by centrifugation, resuspended in 100

μL of a 0.5 mg/mL MTT solution in Hanks+Glc, transferred into a 96-well culture microplate, and incubated for 2 h at 26 or 32 °C, for promastigotes or amastigotes, respectively. The reduced formazan was solubilized by the addition of an equal volume of 10% (w/v) sodium dodecyl sulfate, incubated overnight at 37 °C, and then measured in a 450 Bio-Rad microplate reader equipped with a 595 nm filter.

(ii) To measure the inhibition of promastigote proliferation, the 10 μL aliquot of the aforementioned parasite suspension was added to 100 μL of the growth medium. The surviving parasites were allowed to proliferate for 72 h; then, 100 μL of 1 mg/mL MTT in Hanks+Glc was added, and its reduction was assessed as described above. For amastigotes, the inhibition of proliferation was performed as described above, but growth was carried out in their own medium at 32 °C and extended to 5 days. Afterward, the cells were centrifuged, washed with Hanks+Glc, and resuspended in a 0.5 mg/mL MTT solution, and substrate reduction was allowed to proceed for 2 h at 32 °C. All assays were performed in triplicate, and the experiments were repeated at least twice. The results were normalized to those of the corresponding controls in the absence of peptide.

Variation of Membrane Potential of the Promastigotes and Amastigotes. Membrane potential was estimated by the potential-sensitive anionic dye bisoxonol, since its fluorescence increases after its insertion into the hydrophobic matrix of the membrane, once the cell is depolarized. Assays were performed under standard conditions, in the presence of 0.1 μM bisoxonol. Peptides were added at different concentrations, and changes in fluorescence were recorded continuously for ~30 min using a Polarstar Galaxy microplate reader (BMG Labotechnologies, Offenburg, Germany), equipped with excitation and emission filters at 540 and 580 nm, respectively. Maximal depolarization was considered as that obtained with 2.5 μM CA(1−8)M(1−18) cecropin A−melittin hybrid (*29*). All assays were carried out in triplicate.

Permeation of the Plasma Membrane of the Parasite to the Vital Dye SYTOX Green. To assess the permeability of the *Leishmania* plasma membrane, the entrance of SYTOX Green into the cell was assayed (*35*). Briefly, the parasites were incubated with the peptide according to the standard conditions, with the exception of the addition of 1 μM SYTOX Green (final concentration) into the incubation medium prior to addition of the peptide to equilibrate the parasites with the dye (15 min in darkness). Once the peptide was added, the increase in fluorescence, due to the binding of the dye to intracellular nucleic acids, was measured in the same microplate reader described above, using 485 and 520 nm filters for excitation and emission, respectively. The maximal membrane permeation was defined as that obtained after the addition of 0.1% Triton X-100 (*8*).

Electron Microscopy. Parasites were incubated with the peptides for 1 h and washed twice with phosphate-buffered saline (PBS). Afterward, parasites were fixed for 1 h with 5% (w/v) glutaraldehyde in PBS, included with 2.5% (w/v) osmium tetraoxide, and gradually dehydrated in ethanol [30, 50, 70, 90, and 100% (v/v), 30 min each] and propylene oxide (1 h). Finally, samples were embedded in Epon 812 resin (Tousimis Research Corp., Rockville, MD) and observed with a Philips 2200 electron microscope, as described in previous protocols (*29*).

Statistical Methods. The number of experiments analyzed is indicated in each figure legend. The ED_{50}, defined as the concentration of peptide that inhibits by 50% the MTT reduction compared with the untreated parasites, with its 95% confidence interval, was calculated by the Lichtfield and Wilcoxon procedure, using PHARM-PCS version 4.

ATR-FTIR Measurements. Spectra were obtained with a Bruker equinox 55 FTIR spectrometer equipped with a deuterated triglyceride sulfate detector and coupled to an ATR device as previously described (*36*). Briefly, a mixture of lipids (0.5 mg) alone or with peptide (~20 μg) was deposited on a ZnSe horizontal ATR prism (80 mm × 7 mm). The aperture angle of 45° yielded 25 internal reflections. Prior to sample preparation, the trifluoroacetate counterions, which strongly associate with the peptides, were replaced with chloride ions through several lyophilizations of the peptides in 0.1 M HCl to eliminate an absorption band near 1673 cm^{-1} (*37*). Lipid/peptide mixtures were prepared by dissolving both components together in a 1:2 MeOH/CH$_2$Cl$_2$ mixture and drying them under a stream of dry nitrogen while moving a Teflon bar back and forth along the ZnSe prism. Spectra were recorded, and the respective pure phospholipid spectra were subtracted to yield the difference spectra. The background for each spectrum was a clean ZnSe prism. We hydrated the sample by introducing excess D$_2$O into a chamber placed on top of the ZnSe prism in the ATR casting and incubating the sample for 2 h before acquisition of the spectra. The H−D exchange was considered complete after a total shift of the amide II band. Any contribution of D$_2$O vapor to the absorbance spectra near the amide I peak region was eliminated by subtracting the spectra of pure lipids equilibrated with D$_2$O under the same conditions.

ATR-FTIR Data Analysis. Prior to curve fitting, a straight baseline passing through the ordinates at 1700 and 1600 cm^{-1} was subtracted. To resolve overlapping bands, the spectra were processed using PEAKFIT (Jandel Scientific, San Rafael, CA). Fourth-derivative spectra accompanied by 13-data point Savitsky−Golay smoothing were calculated to identify the positions of the component bands in the spectra. These wavenumbers were used as initial parameters for curve fitting with Gaussian component peaks. The position, bandwidths, and amplitudes of the peaks were varied until (i) the resulting bands shifted by no more than 2 cm^{-1} from the initial parameters, (ii) all the peaks had reasonable half-widths (<20−25 cm^{-1}), and (iii) good agreement between the calculated sum of all the components and the experimental spectra was achieved (r^2 > 0.99). The relative contents of the different secondary structure elements were estimated by dividing the areas of individual peaks, assigned to a specific secondary structure, by the whole area of the resulting amide I band. The results of four independent experiments were averaged. The ATR electric fields of incident light were calculated as previously described (*38, 39*). Lipid order parameters were obtained from the symmetric (~2853 cm^{-1}) and antisymmetric (~2922 cm^{-1}) lipid stretching mode (*39*).

CD Spectroscopy. CD spectra of the peptides were recorded with an Aviv 202 CD spectrophotometer after calibrating the instrument with (+)-10-camphorsulfonic acid. The spectra were scanned at 25 °C in a capped, quartz optical cell with a path length of 0.5 mm. Spectra were obtained at

wavelengths from 260 to 195 nm. The parameters used for the Aviv instrument were as follows: integration time of 8 s, bandwidth of 1 nm, and step size of 1 nm. To quantify the different structures that were obtained, the CD spectra were processed using PEAKFIT (Jandel Scientific). The spectra accompanied by 13-data point Savitsky−Golay smoothing were calculated to identify the positions of the component bands in the spectra. Estimation of secondary structure was carried out as previously described (*40*). More specifically, the CD spectra of the secondary structural elements were used to fit the experimental spectra using a nonlinear least-squares fitting algorithm. The best fit gave the percentage of α-helix, β-strand, β-turn, and unordered structures in each peptide.

Binding Analysis with a Surface Plasmon Resonance (SPR) Biosensor. Biosensor experiments were carried out with a BIAcore 3000 analytical system (Biacore, Uppsala, Sweden) using an L1 sensor chip (BIAcore). The chip is composed of a carboxymethyldextran hydrogel derivatized with lipophilic alkyl chain anchors. Vesicles are passed across this surface and are captured (*41*, *42*). We performed the protocol described by Aguilar et al. (*43*). Briefly, PBS (pH 6.8) was always used as the running buffer; the washing solution was 40 mM octyl glucoside (OG), and the regenerating solution was 10 mM NaOH. All solutions were freshly prepared, degassed, and filtered through 0.22 μm pores. Experiments were carried out at 25 °C. After the BIAcore 3000 instrument was cleaned according to the manufacturer's instructions, it was left running overnight using Milli-Q water as the eluent to thoroughly wash all liquid-handling parts of the instrument. The L1 chip was then installed, and the alkanethiol surface was cleaned by an injection of the nonionic detergent OG (40 mM, 25 μL) at a flow rate of 5 μL/min. PE/PC/PI/PS/erg (4:2:2:1:3, w/w) small unilamellar vesicles (80 μL, 0.5 mM) were then applied to the chip surface at a slow flow rate (2 μL/min). To remove any multilamellar structures from the lipid surface, we injected NaOH (50 μL, 10 mM) at a flow rate of 50 μL/min, which resulted in a stable baseline corresponding to the lipid bilayer linked to the chip surface. The negative control bovine seroalbumin (BSA) was injected (25 μL, 0.1 mg/μL in PBS) to confirm complete coverage of the nonspecific binding sites. The bilayer linked to the chip surface was then used as a model cell membrane surface to study peptide−membrane binding.

Peptide solutions (50 μL of a PBS solution of 0.78−25 μM peptide) were injected onto the lipid surface at a flow rate of 5 μL/min. PBS alone replaced the peptide solution for 30 min to allow peptide dissociation. Surface plasmon resonance detects changes in the reflective index of the surface layer of peptides and lipids in contact with the sensor chip. A sensorgram was obtained by plotting the SPR angle against time. Peptide−lipid binding was analyzed from a series of sensorgrams collected at different peptide concentrations.

The sensorgrams for each peptide−lipid bilayer interaction (L1 chip) were analyzed by curve fitting using numerical integration analysis (*44*). The BIAevaluation software offers different reaction models for performing complete kinetic analyses of the peptide sensorgrams. One curve fitting algorithm (the two-state reaction model) was chosen on the basis of what was known about the possible binding mechanisms of lytic peptides (*31*). The data were fitted globally by simultaneously fitting the peptide sensorgrams obtained at different peptide concentrations. The two-state reaction model was applied to each data set. This model describes two reaction steps (*43*) which, in terms of peptide−lipid interaction, correspond to

$$ P + L \underset{k_{d1}}{\overset{k_{a1}}{\rightleftharpoons}} PL \underset{k_{d2}}{\overset{k_{a2}}{\rightleftharpoons}} PL^* $$
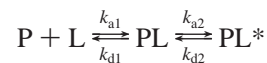
where in the first step peptide (P) binds to lipids (L) to yield PL, which is changed to PL* in the second step. PL* cannot dissociate directly to P and L and may correspond to partial insertion of the peptide into the lipid bilayer. The corresponding differential rate equations for this reaction model are represented by

$$ dRU_1/dt = k_{a1}C_A(RU_{max} - RU_1 - RU_2) - k_{d1}RU_1 - k_{a2}RU_1 + k_{d2}RU_2 $$

$$ dRU_2/dt = k_{a2}RU_1 - k_{d2}RU_2 $$

where RU_1 and RU_2 are the response units for the first and second steps, respectively, C_A is the peptide concentration, RU_{max} is the maximal response unit (or equilibrium binding response), and k_{a1}, k_{d1}, k_{a2}, and k_{d2} are the association and dissociation rate constants for the first and second steps, respectively. k_{a1} has units of M^{-1} s^{-1}, and k_{d1}, k_{a2}, and k_{d2} have units of s^{-1}. Thus, the total affinity constant for the entire process, K, has units of M^{-1}.

RESULTS

Biological Studies

Killing of Leishmania by Bombinins H2 and H4. Bombinins H2 and H4 were tested for their ability to inhibit MTT reduction in *Leishmania* promastigotes and amastigotes over a concentration range of 0.5−25 μM. The assay was done either after a 1 h incubation of the parasites with the peptides (short-term effect) or after proliferation of the remaining viable protozoa via incubation for 3 and 5 days for promastigotes and amastigotes, respectively. Figure 1 shows the results of the inhibition of MTT reduction in promastigotes (panel A) or amastigotes (panel B) for both short- and long-term effects. The data reveal that the two peptides do possess leishmanicidal activity on both forms of the parasite, since a significant overlapping for the two effects was discerned.

Another important conclusion is that up to 10 μM, the loss of parasite viability caused by the H4 diastereomer was consistently higher than with H2. This difference is especially noted for promastigotes, where the values for ED_{50} (the concentration required to inhibit 50% of the MTT reduction compared to that in the untreated parasites) are 7.3 μM (6.6−7.8) and 1.7 μM (0.8−3.4) for bombinins H2 and H4, respectively. For amastigotes, this difference is lower, with ED_{50} values of 11.0 μM (7.3−16.5) and 5.6 μM (3.4−9.4) for H2 and H4, respectively. This trend in activity mirrors the disparity previously found for the bactericidal activity of these two peptides (*22*). Notably, they were devoid of toxic effects on human erythrocytes up to the maximal concentration that was used (data not shown).

The leishmanicidal activity of H2 and H4 was further tested under four different incubation conditions: (i) tem-
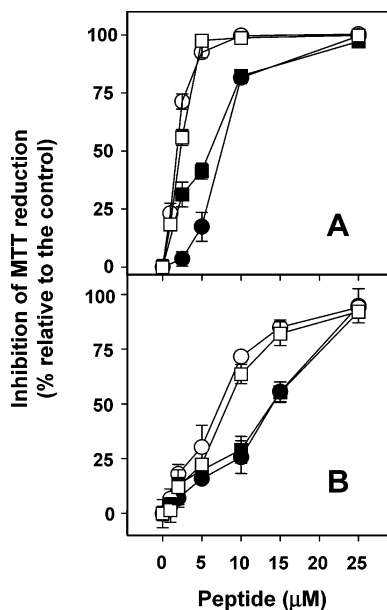
FIGURE 1: Activity of bombinins H2 and H4 on *Leishmania*. The inhibition of MTT reduction by the parasites caused by H2 (filled symbols) or H4 (empty symbols) was assessed, either immediately after the peptide incubation, as representative of the short-term effect (squares), or after allowing the surviving parasites to proliferate (circles), as described in Materials and Methods. (A) *L. donovani* promastigotes and (B) *L. pifanoi* amastigotes. Data are expressed as means ± standard deviations. Data represent the results of a single experiment as representative of three independent ones.

perature, (ii) in the presence of serum, (iii) at different ionic strengths, and (iv) in the presence of polyanions.

(i) The peptide activity was highly dependent on the temperature. Indeed, when bombinins H were assayed at roughly equipotent concentrations for the short-term effect in promastigotes, the percentages of inhibition for H2 (9.0 μM) and H4 (2.5 μM) were 81.3 ± 1.2 and 71.3 ± 6.5% at 26 °C and 2.2 ± 0.5 and 12.4 ± 3.2% at 4 °C, respectively, whereas a complete inhibition of MTT reduction was obtained, in both cases, at 32 °C.

(ii) Bombinins H were shown to be scarcely affected by the presence of human serum up to a concentration of 33% (data not shown). However, in this study, when they were assayed at their ED$_{50}$ values on promastigotes, the addition of 1 mg/mL fatty acid-free seroalbumin decreased the level of inhibition of MTT reduction by H2 from 53.4 ± 3.7 to 32.0 ± 2.1% and that by H4 from 46.2 ± 4.5 to 26.2 ± 3.2%. These results confirmed the importance of the hydrophobicity of the peptides for their microbicidal activity. A possible explanation is that in full serum the proteins that bind hydrophobic molecules are already associated with the fatty acids or other hydrophobic compounds and are not available to bind the peptides. In contrast, in the absence of fatty acids and other serum components, the seroalbumin is free to bind H2 and H4 and hence to reduce their potency.

(iii) The ionic strength of the extracellular medium may impair the electrostatic interaction between cationic peptides and the acidic phospholipids of the outer leaflet of the membrane (29). In *Leishmania*, the substitution of NaCl (140 mM) for 280 mM D-sorbitol in Hanks+Glc gave rise to a strong reduction of the ionic strength of the medium while maintaining isosmoticity; nevertheless, when the two bombinins were assayed against *L. donovani* promastigotes at

their corresponding ED$_{50}$ values in the D-sorbitol medium, the increase in activity was less than 5% for both of them. The peptides were also incubated for 15 min in the presence of heparin (100 μg/mL), a strongly polyanionic polysaccharide that favors the formation of a peptide−polyanion complex, prior to their addition into the parasite suspension. In the absence of heparin, H2 at 10 μM and H4 at 2.5 μM caused an inhibition of MTT reduction of 76.3 ± 3.1 and 72.1 ± 5.4%, respectively, whereas in the presence of this polyanion, these percentages were almost the same, 68.2 ± 1.4 and 64.9 ± 6.4%, respectively.

The insensitivity of H2 and H4 to polyanions prompted us to check the role of the lipophosphoglycan (LPG), the main anionic polysaccharide on the cell surface of promastigotes (45), as a defensive barrier against the two bombinins. For this purpose, we used the promastigotes from the *L. donovani* R2D2 strain (32) (see Materials and Methods) that expressed a truncated form of LPG, mostly devoid of its anionic groups. The ED$_{50}$ values of H2 and H4 were 6.7 μM (5.4−8.3) and 1.3 μM (0.9−1.45), respectively. Thus, the expression of LPG did not protect *Leishmania* against the two peptides.

Permeation of the Plasma Membrane of the Parasites. Previous studies on the bactericidal mechanisms of bombinins H on bacteria (22) revealed that the permeation of the plasma membrane of the pathogen was an essential step in their killing mechanism. To test whether this mechanism could also be extended to their leishmanicidal activity, we assessed the membrane alteration and disruption of the parasite cell by two complementary assays: (i) the plasma membrane's depolarization and (ii) the entrance of vital dyes into the cells, otherwise excluded from intact membranes. Membrane depolarization was followed by monitoring the increase in bisoxonol fluorescence (a potential-sensitive dye) after addition of peptide. Figure 2 shows the kinetics of this process at both stages of the parasite. The data reveal that the two isomers cause a rapid and dose-dependent dissipation of the membrane potential, reaching the end point less than 5 min after peptide addition. In agreement with their activity in the inhibition of promastigote proliferation, bombinin H4, at 5 μM, caused a level of plasma membrane depolarization approaching the maximal value (Figure 2C), whereas a similar result required 25 μM bombinin H2 (Figure 2A). In comparison, closer values for the percentages of depolarization were obtained against amastigotes for H2 and H4 at a given peptide concentration (Figure 2B,D). These results mirrored the effect of the peptides on parasite viability, since the differences between the two isomers were higher on promastigotes than on amastigotes.

To gain insight into the extent of membrane distortion induced by the peptides, we assessed the entrance of SYTOX Green into the cells. This cationic dye (MW = 600) experiences an increase in its fluorescence when bound to intracellular nucleic acids. A marked enhancement in fluorescence was observed within a few minutes of addition of the peptide to the parasites (Figure 3). As in the previous assays, for a given concentration, the effect of H4 was consistently stronger than the effect of H2 on promastigotes (Figure 3A,C), whereas on isolated amastigotes, a dramatic difference was observed at only 10 μM (Figure 3B,D).

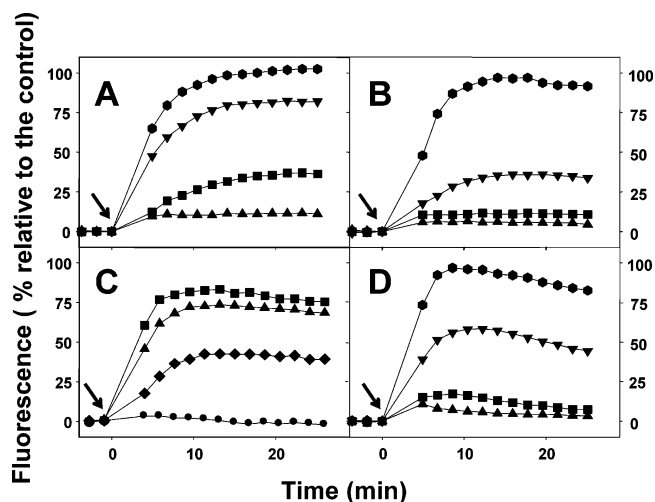*Transmission Electron Microscopy.* We used transmission electron microscopy to visualize the damage inflicted by the

FIGURE 2: Depolarization of the *Leishmania* plasma membrane by bombinins H2 and H4. Parasites (2×10^7 cells/mL) were equilibrated with 0.1 μM bisoxonol at 26 °C. Peptides were then added ($t = 0$) at the corresponding concentrations, and changes in fluorescence were monitored continuously ($\lambda_{\text{exc}} = 540$ nm, $\lambda_{\text{ems}} = 580$ nm) and plotted as the percentage of the total fluorescence relative to maximal parasite depolarization [as achieved by 2.5 μM CA(1$-$8)M(1$-$18)]. All readings were normalized by subtracting parasite scattering and the basal fluorescence of the dye: (A and C) bombinins H2 and H4 on promastigotes and (B and D) bombinins H2 and H4 on amastigotes. The peptide concentrations were 0.5 (●), 1 (◆), 2 (▲), 5 (■), 10 (▼), and 25 μM (⬢). The arrow indicates the addition of peptide. The values are the means of triplicate samples from a single experiment, representative of three separate experiments.
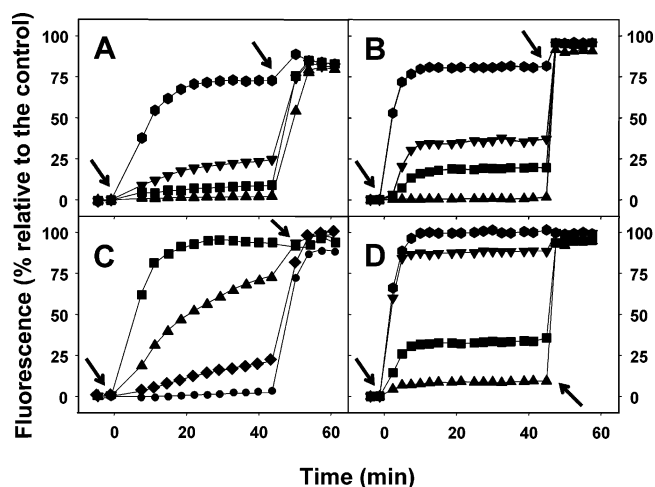

FIGURE 3: Influx of the vital dye SYTOX Green into *Leishmania* promastigotes and amastigotes following the addition of bombinins H. Parasites (2×10^7 cells/mL) were incubated according to the standard assay with 1 μM SYTOX Green in Hanks+Glc. Once basal fluorescence reached a constant value, peptides at the corresponding concentrations were added (first arrow, $t = 0$), and the increase in fluorescence was monitored ($\lambda_{\text{exc}} = 485$ nm, $\lambda_{\text{ems}} = 520$ nm) and plotted as the percentage of fluorescence, relative to that of parasites fully permeated by 0.1% Triton X-100 (final concentration). All readings were normalized by subtracting parasite scattering and the basal fluorescence of the dye: (A and C) bombinins H2 and H4 on promastigotes and (B and D) bombinins H2 and H4 on amastigotes. The peptide concentrations were 0.5 (●), 1 (◆), 2 (▲), 5 (■), 10 (▼), and 25 μM (⬢). The second arrow ($t = 45$ min) indicates the addition of 0.1% Triton X-100. The values are the means of triplicate samples from a single experiment, representative of three different experiments.

peptides on the parasite. Figure 4 illustrates the changes in parasite morphology after its incubation with the two

bombinins H at equipotent concentrations; for the sake of clarity, we show the pictures of amastigotes treated with H2 and H4 at concentrations causing an ∼30% decrease in parasite viability and promastigotes at concentrations causing ∼80% mortality. At low concentrations, most of the parasites appeared with extensive membrane blebbing and increased intracellular vacuolization. At concentrations producing a higher rate of mortality, many parasites became completely permeated, manifested by a loss of electron dense intracellular space and a loss of the shape of cytoplasmic organelles, regardless of the peptide or form of the parasite that was examined.

Biophysical Studies

To account for the biophysical basis of the quantitative differences observed between the two diastereomers, we employed several biophysical techniques that addressed (i) the peptides' structure when bound to different membranes, (ii) the ability of the peptides to perturb the lipid and change its packing, and (iii) differences in the binding affinities of the two peptides for the model phospholipids mimicking the composition of the membrane of *L. donovani* promastigotes.

(i) Secondary Structure of the Peptides in Phospholipid Membranes As Determined by FTIR and CD Spectroscopies. The secondary structure of the peptides was determined in three types of phospholipid multibilayers: (i) PC/cho (10:1, w/w), (ii) PE/PG (7:3, w/w), and (iii) PE/PC/PI/PS/erg (4: 2:2:1:3, w/w). These models served to mimic the composition of the outer leaflet of mammalian erythrocytes, that of the bacterial inner membrane, and that of the plasma membrane of the *L. donovani* promastigotes (*46*), respectively. The amide I region spectra of bombinins H2 and H4 bound to PE/PC/PI/PS/erg multibilayers (after deuterium exchange) are shown as examples, in panels A and B of Figure 5, respectively. Fourth derivatives, accompanied by 13-data point Savitsky$-$Golay smoothing, were calculated to identify the positions of the component bands in the spectra. These wavenumbers were used as initial parameters for curve fitting with Gaussian component peaks. Assignment of the different secondary structures to the various amide I regions was carried out according to the values taken from refs *47*$-$*53*. The relative areas assigned to the corresponding structures of the peptides in PC/cho, PE/PG, and PE/PC/PI/PS/erg multibilayers are summarized in Table 1. As expected, the presence of a D-amino acid at the second position in the bombinin H4 sequence reduced only slightly the helical structure content, compared with that of H2. Interestingly, more pronounced differences were noted in PC/cho and *Leishmania* mimetic PE/PC/PI/PS/erg membranes. Bombinin H4 was found to be significantly less aggregated than H2, which adopted 15 and 30% aggregated β-sheet structure in PC/cho and PE/PC/PI/PS/erg multibilayers, respectively (Table 1). The results obtained at peptide:lipid molar ratios of 1:120 and 1:60 were rather similar.

The structures of the peptides were also determined, by using CD spectroscopy, in buffer and vesicles. The peptides were scanned at 10 μM in PBS and in the presence of PC/ cho, PE/PG, and PE/PC/PI/PS/erg SUVs (2 mM) to give a peptide:lipid molar ratio of 1:200. Figure 6 shows the spectra of bombinin H2 (panel A) and bombinin H4 (panel B) dissolved in PBS and PE/PC/PI/PS/erg SUVs (filled sym-
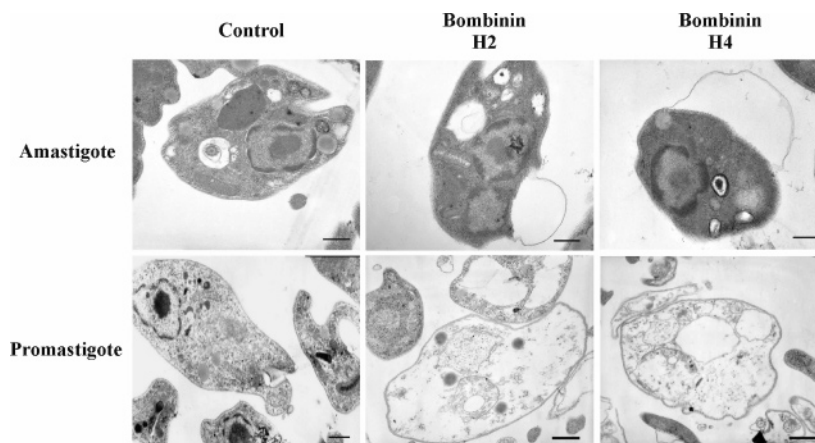
FIGURE 4: Electron microscopy of *Leishmania* promastigotes and amastigotes treated with bombinins H. Axenic *L. pifanoi* amastigotes (top row) and *L. donovani* promastigotes (bottom row) were incubated for 1 h under standard conditions with bombinins H2 and H4 at the equipotent concentrations causing approximately 30 or 80% killing of amastigotes or promastigotes, respectively. The values of the peptide concentrations were determined according to the results reported in Figure 1 (bar = 0.5 μm).

Table 1: Peptide Structures in Lipids As Determined by ATR-FTIR[a] and CD[b] Spectroscopies

peptide	lipid composition	α-helix (%)	aggregated strands (%)	β-sheet (+antiparallel β-sheet) (%)	random coil	lipid order[c]
bombinin H2	PC/cho	65 ± 2 (58 ± 3)	15 ± 1	14 ± 1 (28 ± 1)	6 ± 2 (14 ± 1)	0.03
	PE/PG	75 ± 2 (63 ± 3)	−	18 ± 1 (24 ± 3)	7 ± 1 (13 ± 1)	0.11
	PE/PC/PI/PS/erg	47 ± 1 (50 ± 3)	30 ± 1	14 ± 2 (35 ± 1)	9 ± 1 (15 ± 2)	0.18
bombinin H4	PC/cho	63 ± 3 (55 ± 2)	−	22 ± 1 (23 ± 3)	15 ± 2 (22 ± 2)	0.01
	PE/PG	57 ± 2 (57 ± 4)	−	33 ± 2 (25 ± 2)	10 ± 2 (18 ± 2)	0.01
	PE/PC/PI/PS/erg	55 ± 1 (60 ± 3)	4 ± 1	32 ± 2 (24 ± 3)	9 ± 1 (16 ± 2)	0.10

[a] Lipid:peptide molar ratios of 120:1 and 200:1 were used for FTIR and CD experiments, respectively. The results are the average of four independent experiments. [b] CD results are in parentheses. [c] Lipid order = $R[v_{\text{antisym}}(\text{CH}_2)](\text{lipid} + \text{peptide}) - R[v_{\text{antisym}}(\text{CH}_2)]$.

bols). The spectra of the peptides in PC/cho and PE/PG SUVs are similar to their spectra in PE/PC/PI/PS/erg SUVs and therefore are not shown. The structural components of both peptides when bound to the three types of lipid vesicles are also shown in Table 1 (in parentheses). Importantly, the structural components determined by using CD spectroscopy are similar to those obtained by FTIR. Note that the β-sheet structure content is shown as the sum of the parallel and antiparallel components.

(ii) Orientation of the Phospholipid Membrane and Effect of the Peptides on the Phospholipid Acyl Chain Order. Polarized ATR-FTIR spectroscopy was used to determine the orientation of the lipid membrane with or without the bound peptides. The symmetric $[v_{\text{sym}}(\text{CH}_2) \approx 2853 \text{ cm}^{-1}]$ and antisymmetric $[v_{\text{sym}}(\text{CH}_2) \approx 2922 \text{ cm}^{-1}]$ vibrations of lipid methylene C−H bonds are perpendicular to the molecular axis of a fully extended hydrocarbon chain. Thus, measuring the dichroism of infrared light absorbance can reveal the order and orientation of the membrane sample relative to the prism surface. The effect of the peptides on the acyl chain order was estimated by comparing the CH$_2$ stretching dichroic ratio of phospholipid (with different compositions) multibilayers alone with that obtained with membrane-bound peptides. The most significant difference was observed in PE/PC/PI/PS/erg membranes. The calculated values, based on the antisymmetric vibrations of the peptide-bound membrane minus membrane alone, were found to be 0.18 and 0.10 for H2 and H4, respectively (Table 1). Similar results were observed on the basis of the symmetric vibrations. Thus, the data revealed that the incorporation of bombinin H2 has a more pronounced effect on the acyl chain
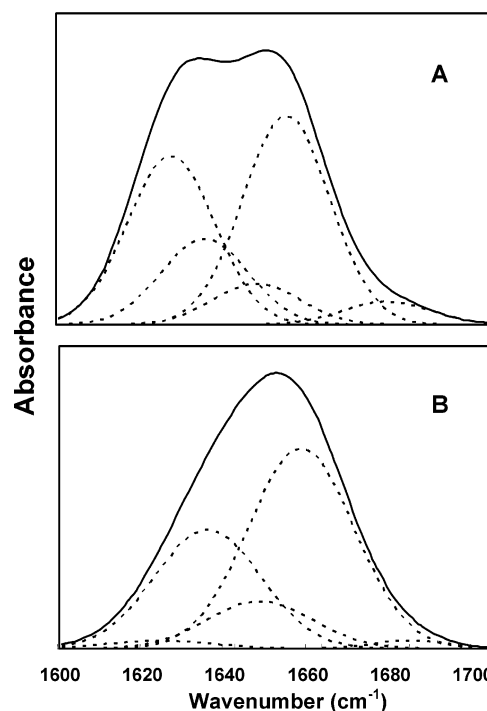

FIGURE 5: FTIR spectral deconvolution of the fully deuterated amide I band (1600−1700 cm^{-1}) of bombinin H2 (A) and bombinin H4 (B) in PE/PC/PI/PS/erg (4:2:2:1:3, w/w) multibilayers. The component peaks are the result of curve fitting using a Gaussian line shape. The sums of the fitted components superimpose on the experimental amide I region spectra. Bold lines represent the experimental FTIR spectra after Savitzky−Golay smoothing; the dotted lines represent the fitted components. A lipid:peptide molar ratio of 120:1 was used.
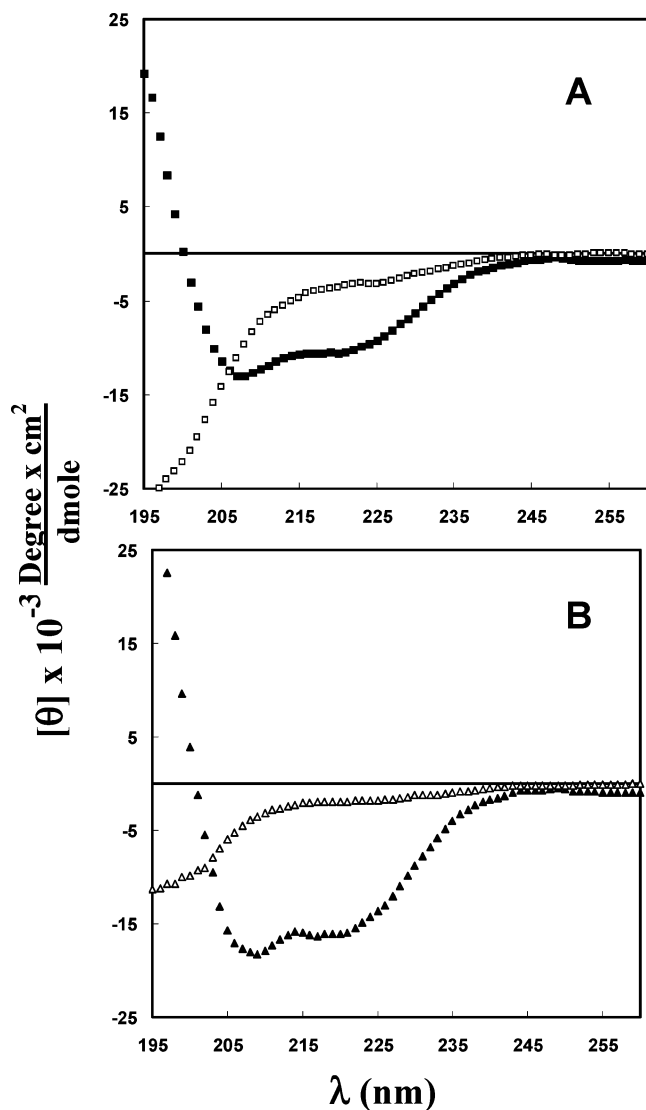
FIGURE 6: CD spectra of bombinin H2 (A) and bombinin H4 (B) peptides. Spectra were taken at 10 μM peptide dissolved in PBS (empty symbols) and 2 mM PE/PC/PI/PS/erg SUVs (filled symbols). The spectra of the peptides in PC/cho and PE/PG SUVs overlap the spectra in PE/PC/PI/PS/erg SUVs and therefore are not shown.
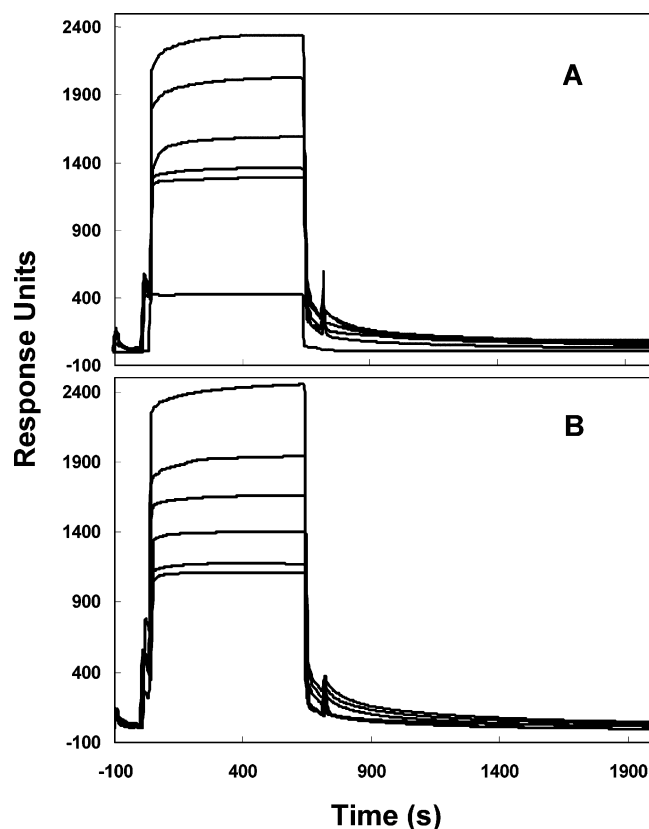

FIGURE 7: Sensorgrams of the binding between various concentrations of bombinin H2 (A), bombinin H4 (B), and the PE/PC/PI/PS/erg (4:2:2:1:3, w/w) lipid bilayer (using an L1 sensor chip). Concentrations of the peptides from bottom to top were 0.78, 1.56, 3.125, 6.25, 12.5, and 25 μM.

Table 2: Constants for Binding of Peptides to PE/PC/PI/PS/erg Bilayers Determined by Numerical Integration Using a Two-State Reaction Model[a]

peptide	K_1 (M^{-1})	K_2	K (M^{-1})
bombinin H2	1.5×10^5	1.5	$(2.2 \pm 0.1) \times 10^5$
bombinin H4	7.3×10^5	1.4	$(9.9 \pm 0.4) \times 10^5$

[a] The binding constants K_1 and K_2 are for the first ($K_1 = k_{a1}/k_{d1}$) and second ($K_2 = k_{a2}/k_{d2}$) binding steps, respectively, and the affinity constant (K), which equals $K_1 K_2$, is for the complete binding process.

order of the *Leishmania* mimetic membranes than that of H4 does.

(iii) Binding Affinity of the Peptides for Lipid Bilayers Measured by Surface Plasmon Resonance: A Two-State Model for the Binding of the Peptide to Membranes. Typical sensorgrams of the binding of H2 and H4 to PE/PC/PI/PS/erg bilayers are shown in panels A and B of Figure 7, respectively. We employed numerical integration analysis which uses nonlinear analysis to fit an integrated rate equation directly to the sensorgrams (*43*). When fitting the peptide's sensorgrams globally (using different concentrations of the peptides) with the simplest 1:1 Langmuir binding model, we produced a poor fit (data not shown), confirming that this model does not represent the lipid binding mechanism of all the peptides that were investigated. However, a significantly improved fit was obtained by using numerical integration of the two-state reaction model of the binding sensorgrams. This model reflects a two-step process in the interaction of the peptides with lipid bilayers: the first step is the actual binding, and the second step is the insertion of

the peptide into the membrane. A set of peptide sensorgrams with different peptide concentrations was used to estimate the kinetic parameters. The average values for the rate constants obtained from the two-state model analysis are listed in Table 2 along with the binding constant values (K). The data confirm that bombinin H4 has a higher affinity than H2 for the PE/PC/PI/PS/erg bilayers (K, Table 2), which is the result of the first step (K_1, Table 2). In contrast, both peptides have similar partitioning constants (K_2, Table 2) in the second step (insertion step).

DISCUSSION

The presence of a D-amino acid in peptides of animal origin was first identified in dermorphin and deltorphins, opioid peptides isolated from the skin of South American frogs *Phyllomedusa sauvagei* and *Phyllomedusa bicolor* (*54, 55*), and subsequently in other neuropeptides from invertebrates (*56–59*). However, although D-amino acids are found in the sequence of bacterial or fungal AMPs, as a conse-

quence of nonribosomal synthesis (*60*), H4 and H7 are two exclusive examples of such a modification reported to date for AMPs in vertebrates (*18*), in which the D-amino acid is formed as a result of a post-translational process by epimerization of the pre-existing L-amino acid. The enzyme responsible for this L−D isomerization has been purified and characterized very recently (*21*).

We found that bombinins H2 and H4 are active on the insect and the mammalian forms of *Leishmania* at a micromolar concentration range (without being toxic to human erythrocytes) and that they rapidly perturb their plasma membrane; actually, treated parasites exhibited the typical pattern described for other membrane-active peptides (*8*, *29*, *35*, *61*, *62*), with an extensive blebbing. Increasing the peptide concentration led to massive destruction of parasites and loss of intracellular material, with blurred definition of the boundaries of the intracellular organelles. In functional terms, the peptides caused a rapid depolarization and loss of integrity of the plasma membrane, together with a rapid bioenergetic collapse. All these processes took place simultaneously with the inhibition of parasite proliferation in a very short time (within minutes) and in a concentration-dependent manner. These findings also correlated with the extent of that inhibition.

The leishmanicidal activity that was detected for bombinins H is in the same range as those of other AMPs that act on membranes (*3*, *5*). However, an interesting result is the improved leishmanicidal activity caused by a single residue epimerization of bombinin H2, especially with regard to promastigotes. To better understand the parameters of the peptides underlying this observation, we employed several microbiological and physicochemical experimental procedures.

Differences in Susceptibilities to Enzymatic Degradation. Inclusion of D-amino acids in the sequence of AMPs has been shown to protect them from enzymatic degradation and serum clearance (*63−65*). Here, differences in the susceptibility to enzymatic degradation do not seem to be important for the following reasons. (i) *Leishmania* is an organism that is especially endowed with peptidase and proteinase activities (*66*). However, only a couple of metallo aminopeptidases have been well-characterized (*67*); they preferentially recognize leucine residues but act very poorly on isoleucine, the N-terminal residue of H2 and H4. (ii) When promastigotes were incubated for 1 h, prior to the addition of the peptides with 2 mM EDTA, a treatment that inhibited the activity of these two aminopeptidases and that of the metalloproteinase, leishmaniolysin (*68*), no significant difference in activity was discerned between H2 and H4 (data not shown). (iii) The time available for peptide degradation is very short because the final effect on parasite viability is achieved a few minutes after addition of the peptide.

Differences between the Structures and Organization of the Peptides. An alternative way of explaining the different activities of the two isomers could be a variation in their structures, a parameter that has been shown to be important for biological function. Incorporation of D-amino acids within AMPs induced structural changes, and the resulting diastereomers preserved their antimicrobial activity but lost their function on higher eukaryotic cells (reviewed in ref *5*). Bombinin H4 contains a D-alloisoleucine at its second N-terminal position, adjacent to a glycine-proline sequence.

This sequence is known as an α-helix destabilizing motif found as a hinge between two sufficiently long structural domains, as described for cecropin A (*69*). We therefore expected that the structures of H2 and H4 would be similar. Indeed, FTIR and CD studies demonstrated that the overall structures of H2 and H4 are not significantly different (Table 1). However, compared to H4, H2 adopts β-sheet aggregates in the parasite− and erythrocyte−mimetic membranes (30 and 15% aggregated strands, respectively) (Table 1). Although the reason is not yet clear, the formation of aggregated strands by H2 could contribute to its lower activity against *Leishmania* compared to that of H4.

The ability of AMPs to kill microorganisms also depends on their potential to perturb the membrane. The data revealed that H2 is more potent than its isomer (larger R value) in affecting the lipid order of the three different model membranes, which seems to contradict its lower activity on *Leishmania* compared with that of H4. Nevertheless, many transmembrane peptides can insert into the hydrophobic core of a membrane without affecting its integrity. However, we cannot rule out the possibility that, compared with model membranes, there are physical constraints (i.e., the abundant and bulky glycophosphoinositol anchored components of the plasma membrane of the intact parasite), which may induce mechanical stress and consequently influence the activity of membrane-active AMPs.

Differences in Membrane Binding. We carried out SPR measurements with lipid bilayers to detect differences between the binding affinities of the two bombinins H for the *Leishmania* mimicking membranes. Our results indicate that H4 has a higher affinity than H2 (Table 2), in agreement with its higher hydrophobicity detected by using reverse phase HPLC (*18*). The higher affinity of H4 is due to the first binding step, K_1 (most probably caused by hydrophobic interactions between the more hydrophobic H4 and the zwitterionic membrane), and not because of the insertion step, K_2, which is similar for both of them, and which characterizes antimicrobial peptides that act via the carpet mechanism (*31*). Overall, these data suggest that H2 has a stronger effect on the lipid order (as revealed by FTIR studies), not because it inserts better than H4, but rather because of its aggregational state when it is in contact with the membrane. The findings that a decrease in the ionic strength, as well as the preincubation of the peptides with heparin, did not markedly influence their activity and that incubation with BSA reduced it by 50% further support the notion that hydrophobic interactions play a major role in the mode of action of H2 and H4.

Finally, as previously described for the cecropin A−melittin hybrid peptides (*8*) but not for temporins (*35*), we found that amastigotes were more resistant than promastigotes and that the difference in the activities between the two isomers was more pronounced against promastigotes. The most reasonable explanation is the different lipid composition of the plasma membrane of amastigotes compared with that of promastigotes, although only limited data on the variation of some phospholipids through the life cycle of *Leishmania* are currently available (*70*).

In summary, this study demonstrates the importance of a single D-amino acid substitution as a new approach developed by nature to modulate not only the bioavailability (e.g., higher solubility) and biostability (i.e., protection from proteolytic

degradation) of AMPs but also their biophysical properties and antimicrobial activity. In addition, our findings suggest bombinins H as potential templates for the development of new anti-*Leishmania* drugs with a new mode of action urgently needed because of the increased resistance of *Leishmania* to available chemotherapeutic drugs.

ACKNOWLEDGMENT

We thank Vlad Brumfeld for his assistance in the deconvolution of the CD spectra.

REFERENCES

1. Boman, H. G. (1995) Peptide antibiotics and their role in innate immunity, *Annu. Rev. Immun. 13*, 61−92.
2. Zasloff, M. (2002) Antimicrobial peptides of multicellular organisms, *Nature 415*, 389−395.
3. Hancock, R. E. W., and Scott, M. G. (2000) The role of antimicrobial peptides in animal defenses, *Proc. Natl. Acad. Sci. U.S.A. 97*, 8856−8861.
4. Brogden, K. A. (2005) Antimicrobial peptides: Pore formers or metabolic inhibitors in bacteria? *Nat. Rev. Microbiol. 3*, 238−250.
5. Shai, Y. (2002) Mode of action of membrane active antimicrobial peptides, *Biopolymers 66*, 236−248.
6. Cudic, M., and Otvos, L., Jr. (2002) Intracellular targets of antibacterial peptides, *Curr. Drug Targets 3*, 101−106.
7. Avrahami, D., and Shai, Y. (2002) Conjugation of a magainin analogue with lipophilic acids controls hydrophobicity, solution assembly, and cell selectivity, *Biochemistry 41*, 2254−2263.
8. Chicharro, C., Granata, C., Lozano, R., Andreu, D., and Rivas, L. (2001) N-Terminal fatty acid substitution increases the leishmanicidal activity of CA(1−7)M(2−9), a cecropin-melittin hybrid peptide, *Antimicrob. Agents Chemother. 45*, 2441−2449.
9. Feder, R., Dagan, A., and Mor, A. (2000) Structure−activity relationship study of antimicrobial dermaseptin S4 showing the consequences of peptide oligomerization on selective cytotoxicity, *J. Biol. Chem. 275*, 4230−4238.
10. Guerrero, E., Saugar, J. M., Matsuzaki, K., and Rivas, L. (2004) Role of positional hydrophobicity in the leishmanicidal activity of magainin 2, *Antimicrob. Agents Chemother. 48*, 2980−2986.
11. Sal-Man, N., Oren, Z., and Shai, Y. (2002) Preassembly of membrane-active peptides is an important factor in their selectivity toward target cells, *Biochemistry 41*, 11921−11930.
12. Barra, D., and Simmaco, M. (1995) Amphibian skin: A promising resource for antimicrobial peptides, *Trends Biotechnol. 13*, 205−209.
13. Bevins, C. L., and Zasloff, M. (1990) Peptides from frog skin, *Annu. Rev. Biochem. 59*, 395−414.
14. Nicolas, P., and Mor, A. (1995) Peptides as weapons against microorganisms in the chemical defense system of vertebrates, *Annu. Rev. Microbiol. 49*, 277−304.
15. Mangoni, M. L., Miele, R., Renda, T. G., Barra, D., and Simmaco, M. (2001) The synthesis of antimicrobial peptides in the skin of *Rana esculenta* is stimulated by microorganisms, *FASEB J. 15*, 1431−1432.
16. Gibson, B. W., Tang, D. Z., Mandrell, R., Kelly, M., and Spindel, E. R. (1991) Bombinin-like peptides with antimicrobial activity from skin secretions of the Asian toad, *Bombina orientalis*, *J. Biol. Chem. 266*, 23103−23111.
17. Simmaco, M., Barra, D., Chiarini, F., Noviello, L., Melchiorri, P., Kreil, G., and Richter, K. (1991) A family of bombinin-related peptides from the skin of *Bombina variegata*, *Eur. J. Biochem. 199*, 217−222.
18. Mignogna, G., Simmaco, M., Kreil, G., and Barra, D. (1993) Antibacterial and haemolytic peptides containing D-alloisoleucine from the skin of *Bombina variegata*, *EMBO J. 12*, 4829−4832.
19. Kreil, G. (1997) D-Amino acids in animal peptides, *Annu. Rev. Biochem. 66*, 337−345.
20. Mor, A., Amiche, M., and Nicolas, P. (1992) Enter a new posttranslational modification: D-Amino acids in gene-encoded peptides, *Trends Biochem. Sci. 17*, 481−485.
21. Jilek, A., Mollay, C., Tippelt, C., Grassi, J., Mignogna, G., Mullegger, J., Sander, V., Fehrer, C., Barra, D., and Kreil, G. (2005) Biosynthesis of a D-amino acid in peptide linkage by an

enzyme from frog skin secretions, *Proc. Natl. Acad. Sci. U.S.A. 102*, 4235−4239.
22. Mangoni, M. L., Grovale, N., Giorgi, A., Mignogna, G., Simmaco, M., and Barra, D. (2000) Structure−function relationships in bombinins H, antimicrobial peptides from *Bombina* skin secretions, *Peptides 21*, 1673−1679.
23. Berman, J. (2005) Recent developments in leishmaniasis: Epidemiology, diagnosis, and treatment, *Curr. Infect. Dis. Rep. 7*, 33−38.
24. Croft, S. L., and Coombs, G. H. (2003) Leishmaniasis: Current chemotherapy and recent advances in the search for novel drugs, *Trends Parasitol. 19*, 502−558.
25. Guerin, P. J., Olliaro, P., Sundar, S., Boelaert, M., Croft, S. L., Desjeux, P., Wasunna, M. K., and Bryceson, A. D. (2002) Visceral leishmaniasis: Current status of control, diagnosis, and treatment, and a proposed research and development agenda, *Lancet Infect. Dis. 2*, 494−501.
26. Gull, K. (1999) The cytoskeleton of trypanosomatid parasites, *Annu. Rev. Microbiol. 53*, 629−655.
27. McConville, M. J., Mullin, K. A., Ilgoutz, S. C., and Teasdale, R. D. (2002) Secretory pathway of trypanosomatid parasites, *Microbiol. Mol. Biol. Rev. 66*, 122−154.
28. Ilgoutz, S. C., and McConville, M. J. (2001) Function and assembly of the *Leishmania* surface coat, *Int. J. Parasitol. 31*, 899−908.
29. Diaz-Achirica, P., Ubach, J., Guinea, A., Andreu, D., and Rivas, L. (1998) The plasma membrane of *Leishmania donovani* promastigotes is the main target for CA(1−8)M(1−18), a synthetic cecropin A-melittin hybrid peptide, *Biochem. J. 330*, 453−460.
30. Mangoni, M. L., Rinaldi, A. C., Di Giulio, A., Mignogna, G., Bozzi, A., Barra, D., and Simmaco, M. (2000) Structure−function relationships of temporins, small antimicrobial peptides from amphibian skin, *Eur. J. Biochem. 267*, 1447−1454.
31. Papo, N., and Shai, Y. (2003) Exploring peptide membrane interaction using surface plasmon resonance: Differentiation between pore formation versus membrane disruption by lytic peptides, *Biochemistry 42*, 458−466.
32. King, D. L., and Turco, S. J. (1988) A ricin agglutinin-resistant clone of *Leishmania donovani* deficient in lipophosphoglycan, *Mol. Biochem. Parasitol. 28*, 285−293.
33. Pan, A. A., McMahon-Pratt, D., and Honigberg, B. M. (1984) *Leishmania mexicana pifanoi*: Antigenic characterization of promastigote and amastigote stages by solid-phase radioimmunoassay, *J. Parasitol. 70*, 834−835.
34. Hanks, W. J. (1958) Determination of cell viability, *Proc. Soc. Biol. Med. 98*, 188−192.
35. Mangoni, M. L., Saugar, J. M., Dellisanti, M., Barra, D., Simmaco, M., and Rivas, L. (2005) Temporins, small antimicrobial peptides with leishmanicidal activity, *J. Biol. Chem. 280*, 984−990.
36. Oren, Z., and Shai, Y. (2000) Cyclization of a cytolytic amphipathic α-helical peptide and its diastereomer: Effect on structure, interaction with model membranes, and biological function, *Biochemistry 39*, 6103−6114.
37. Surewicz, W. K., Mantsch, H. H., and Chapman, D. (1993) Determination of protein secondary structure by Fourier transform infrared spectroscopy: A critical assessment, *Biochemistry 32*, 389−394.
38. Harrick, N. J. (1967) *Internal Reflection Spectroscopy*, Interscience, New York.
39. Ishiguro, R., Kimura, N., and Takahashi, S. (1993) Orientation of fusion-active synthetic peptides in phospholipid bilayers: Determination by Fourier transform infrared spectroscopy, *Biochemistry 32*, 9792−9797.
40. Brumfeld, V., and Miller, I. R. (1988) Effect of membrane potential on the conformation of bacterorhodopsin reconstituted in lipid vesicles, *Biophys. J. 54*, 747−750.
41. Erb, E. M., Chen, X., Allen, S., Roberts, C. J., Tendler, S. J., Davies, M. C., and Forsen, S. (2000) Characterization of the surfaces generated by liposome binding to the modified dextran matrix of a surface plasmon resonance sensor chip, *Anal. Biochem. 280*, 29−35.
42. Cooper, M. A., Hansson, A., Lofas, S., and Williams, D. H. (2000) A vesicle capture sensor chip for kinetic analysis of interactions with membrane-bound receptors, *Anal. Biochem. 277*, 196−205.
43. Mozsolits, H., Wirth, H. J., Werkmeister, J., and Aguilar, M. I. (2001) Analysis of antimicrobial peptide interactions with hybrid bilayer membrane systems using surface plasmon resonance, *Biochim. Biophys. Acta 1512*, 64−76.
44. Morton, T. A., Myszka, D. G., and Chaiken, I. M. (1995) Interpreting complex binding kinetics from optical biosensors: A

comparison of analysis by linearization, the integrated rate equation, and numerical integration, *Anal. Biochem. 227*, 176−185.

45. Turco, S. J., Hull, S. R., Orlandi, P. A., Jr., Shepherd, S. D., Homans, S. W., Dwek, R. A., and Rademacher, T. W. (1987) Structure of the major carbohydrate fragment of the *Leishmania donovani* lipophosphoglycan, *Biochemistry 26*, 6233−6238.

46. Wassef, M. K., Fioretti, T. B., and Dwyer, D. M. (1985) Lipid analyses of isolated surface membranes of *Leishmania donovani* promastigotes, *Lipids 20*, 108−115.

47. Byler, D. M., and Susi, H. (1986) Examination of the secondary structure of proteins by deconvolved Fourier transform infrared spectroscopy, *Biopolymers 25*, 469−487.

48. Jackson, M., and Mantsch, H. H. (1995) The use and misuse of FTIR spectroscopy in the determination of protein structure, *Crit. Rev. Biochem. Mol. Biol. 30*, 95−120.

49. Frey, S., and Tamm, L. K. (1991) Orientation of melittin in phospholipid bilayers. A polarized attenuated total reflection infrared study, *Biophys. J. 60*, 922−930.

50. Pezolet, M., Bonenfant, S., Doussau, F., and Papineau, Y. (1992) Conformation of wheat gluten proteins. Comparison between functional and solution states as determined by infrared spectroscopy, *FEBS Lett. 299*, 247−250.

51. Oren, Z., Hong, J., and Shai, Y. (1999) A comparative study on the structure and function of a cytolytic α-helical peptide and its antimicrobial β-sheet diastereomer, *Eur. J. Biochem. 259*, 360−369.

52. Hong, J., Oren, Z., and Shai, Y. (1999) The structure and organization of hemolytic and nonhemolytic diastereomers of antimicrobial peptides in membranes, *Biochemistry 38*, 16963−16973.

53. Sharon, M., Oren, Z., Shai, Y., and Anglister, J. (1999) 2D-NMR and ATR-FTIR study of the structure of a cell-selective diastereomer of melittin and its orientation in phospholipids, *Biochemistry 38*, 15305−15316.

54. Montecucchi, P. C., de Castiglione, R., Piani, S., Gozzini, L., and Erspamer, V. (1981) Amino acid composition and sequence of dermorphin, a novel opiate-like peptide from the skin of *Phyllomedusa sauvagei*, *Int. J. Pept. Protein Res. 17*, 275−283.

55. Erspamer, V., Melchiorri, P., Falconieri-Erspamer, G., Negri, L., Corsi, R., Severini, C., Barra, D., Simmaco, M., and Kreil, G. (1989) Deltorphins: A family of naturally occurring peptides with high affinity and selectivity for delta opioid binding sites, *Proc. Natl. Acad. Sci. U.S.A. 86*, 5188−5192.

56. Kamatani, Y., Minakata, H., Kenny, P. T., Iwashita, T., Watanabe, K., Funase, K., Sun, X. P., Yongsiri, A., Kim, K. H., Novales-Li, P., et al. (1989) Achatin-I, an endogenous neuroexcitatory tetrapeptide from *Achatina fulica* Ferussac containing a D-amino acid residue, *Biochem. Biophys. Res. Commun. 160*, 1015−1020.

57. Buczek, O., Yoshikami, D., Bulaj, G., Jimenez, E. C., and Olivera, B. M. (2005) Post-translational amino acid isomerization: A functionally important D-amino acid in an excitatory peptide, *J. Biol. Chem. 280*, 4247−4253.

58. Kuwada, M., Teramoto, T., Kumagaye, K. Y., Nakajima, K., Watanabe, T., Kawai, T., Kawakami, Y., Niidome, T., Sawada,

K., Nishizawa, Y., et al. (1994) ω-Agatoxin-TK containing D-serine at position 46, but not synthetic ω-[L-Ser46]agatoxin-TK, exerts blockade of P-type calcium channels in cerebellar Purkinje neurons, *Mol. Pharmacol. 46*, 587−593.

59. Torres, A. M., Menz, I., Alewood, P. F., Bansal, P., Lahnstein, J., Gallagher, C. H., and Kuchel, P. W. (2002) D-Amino acid residue in the C-type natriuretic peptide from the venom of the mammal, *Ornithorhynchus anatinus*, the Australian platypus, *FEBS Lett. 524*, 172−176.

60. Mignogna, G., Simmaco, M., and Barra, D. (1998) Occurrence and function of D-amino acid-containing peptides and proteins: Antimicrobial peptides, *EXS 85*, 29−36.

61. Hernandez, C., Mor, A., Dagger, F., Nicolas, P., Hernandez, A., Benedetti, E. L., and Dunia, I. (1992) Functional and structural damage in *Leishmania mexicana* exposed to the cationic peptide dermaseptin, *Eur. J. Cell Biol. 59*, 414−424.

62. Silva, P. I., Jr., Daffre, S., and Bulet, P. (2000) Isolation and characterization of gomesin, an 18-residue cysteine-rich defense peptide from the spider *Acanthoscurria gomesiana* hemocytes with sequence similarities to horseshoe crab antimicrobial peptides of the tachyplesin family, *J. Biol. Chem. 275*, 33464−33470.

63. Papo, N., Oren, Z., Pag, U., Sahl, H. G., and Shai, Y. (2002) The consequence of sequence alteration of an amphipathic α-helical antimicrobial peptide and its diastereomers, *J. Biol. Chem. 277*, 33913−33921.

64. Hong, S. Y., Oh, J. E., and Lee, K. H. (1999) Effect of D-amino acid substitution on the stability, the secondary structure, and the activity of membrane-active peptide, *Biochem. Pharmacol. 58*, 1775−1780.

65. Braunstein, A., Papo, N., and Shai, Y. (2004) In vitro activity and potency of an intravenously injected antimicrobial peptide and its DL amino acid analog in mice infected with bacteria, *Antimicrob. Agents Chemother. 48*, 3127−3129.

66. Mottram, J. C., Coombs, G. H., and Alexander, J. (2004) Cysteine peptidases as virulence factors of *Leishmania*, *Curr. Opin. Microbiol. 7*, 375−381.

67. Morty, R. E., and Morehead, J. (2002) Cloning and characterization of a leucyl aminopeptidase from three pathogenic *Leishmania* species, *J. Biol. Chem. 277*, 26057−26065.

68. Yao, C., Donelson, J. E., and Wilson, M. E. (2003) The major surface protease (MSP or GP63) of *Leishmania* sp. Biosynthesis, regulation of expression, and function, *Mol. Biochem. Parasitol. 132*, 1−16.

69. Holak, T. A., Engstrom, A., Kraulis, P. J., Lindeberg, G., Bennich, H., Jones, T. A., Gronenborn, A. M., and Clore, G. M. (1988) The solution conformation of the antibacterial peptide cecropin A: A nuclear magnetic resonance and dynamical simulated annealing study, *Biochemistry 27*, 7620−7629.

70. Tripathi, A., and Gupta, C. M. (2003) Transbilayer translocation of membrane phosphatidylserine and its role in macrophage invasion in *Leishmania* promastigotes, *Mol. Biochem. Parasitol. 128*, 1−9.